COBEM 99
XV Congresso Brasileiro de Engenharia Mecânica
15th Brazilian Congress of Mechanical Engineering
22 - 26 de Novembro de 1999 / November 22 - 26, 1999 Águas de Lindóia, São Paulo,

A STUDY ON BRITTLE FRACTURE IN PWR VESSELS UNDER PRESSURIZED THERMAL SHOCK WITH ASYMMETRIC REFRIGERATION

Gustavo Benitez Alvarez
Eduardo Gomes Dutra do Carmo
Nilson Costa Roberty
Universidade Federal do Rio de Janeiro, COPPE-Programa de Engenharia Nuclear
Cx. P.68509, CEP 21945-970, Prédio do Centro de Tecnologia, Bloco G Sala 206 Ilha do Fundão, RJ, Brazil

Abstract. *In this study we develop a methodology for mapping operational curves (pressures in the vessel versus cold leg temperature), to avoid brittle fractures under pressurized thermal shock with asymmetric refrigeration. The methodology begins by a thermal analysis of several transients with an asymmetric refrigeration of the beltline region (the fluid temperature of the vessel inner wall depends on theta and the maximum heat transference coefficient is taken for all temperatures). The thermal problem is solved by using a hybrid method of finite elements and a global base for spatial dependency. An implicit scheme of finite differences, as the Euler's, has been used for temporal dependency. Later, a stress analysis was carried out considering a quasi-stationary model. A hybrid method is used, once again, to obtain a thermomechanical stresses profile. Finally, thermomechanical stresses are post-processed to carry out the fracture mechanics analysis using the linear-elastic fracture mechanics model. Operational bounding curves (pressure versus cold leg temperature) are presented for a typical PWR. These curves provide the operators with information related to the plant's safety status concerning the possibility of a brittle fracture in the beltline region.*

Keywords: *Brittle fractures, Thermal shock*

1. INTRODUCTION

The possibility of occurring a pressurized thermal shock on PWR (pressurized water reactor) reactors has been calling a great deal of attention from all companies working with this kind of reactor. The main problem is to avoid brittle fractures on the vase area exposed to sudden drops of temperature associated with high thermal stresses and a raise of RT_{NDT} (Nil-ductility transition reference temperature) due to fast neutrons irradiation.

Thus, to avoid brittle fractures it makes it necessary to obtain curves of admissible pressures against cold leg temperatures.

These curves should contain all possible safety margins and allow the operator some room for maneuver to proceed according to the operation manual' s recommendations.

Carmo, Oliveira and Roberty (1984) developed a methodology to obtain such curves. Still, it does not allow an analysis on the temperature field's asymmetric influence.

This study aims at producing a rough preliminary evaluation about the influence of this asymmetry.

2. METHODOLOGY

The region of the pressure vessel where occur high temperature gradient, increase of RT_{NDT} (Nil-ductility transition reference temperature) and high thermal stress is called the "belt-line" region, which is illustrated on Fig. 1. Therefore, the analysis is carried out in this region.

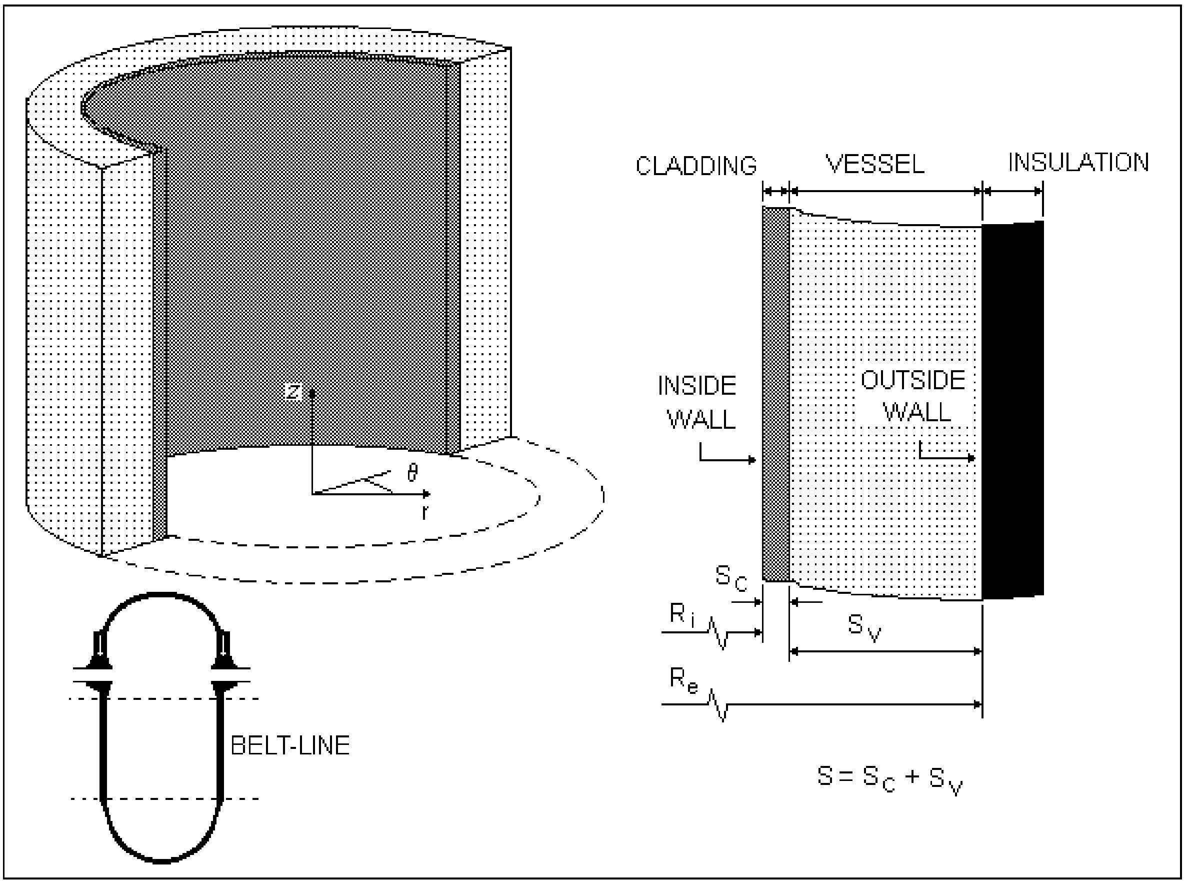

Figure 1-Illustration of belt-line region.

In order to obtain admissible pressures as a function of cold leg temperature, we need the following analyses:

i) thermal analysis of several transients,
ii) thermomechanic stress analysis of several transients,
iii) fracture mechanics analysis.

Two materials as is illustrated in Fig. 1 form the vessel.

2.1 Thermal analysis

The belt-line region is described in cylindrical coordinates by:

$$\Omega = \{(r, \theta, z); \quad R_i < r < R_e, \quad 0 \le \theta \le 2\pi, \quad -\left(\tfrac{H}{2}\right) < z < \left(\tfrac{H}{2}\right)\}, \tag{2.1}$$

where R_i denotes inner radius, R_e denotes outer radius and H is the height of the cylinder.

The initial boundary value problem consists on finding $T = T(r,\theta,z,t)$, $(r,\theta,z) \in \Omega$, $t \in (0,\infty)$, such that:

$$div\left[k\tilde{\nabla}T\right] = \rho\, c_p \frac{\partial T}{\partial t} \text{ in } \Omega, \tag{2.2a}$$

$$T(r,\theta,z,0) = T_{ON} \text{ in } \Omega, \tag{2.2b}$$

$$\frac{\partial T(R_e,\theta,z,t)}{\partial r} = 0, \tag{2.2c}$$

$$\frac{\partial T(r,\theta,\pm\frac{H}{2},t)}{\partial z} = 0, \tag{2.2d}$$

$$k\frac{\partial T(R_i,\theta,z,t)}{\partial r} = h\left[T(R_i,\theta,z,t) - T_f(\theta,z)\right], \tag{2.2e}$$

where $div(\cdot)$ denotes divergent operator, $\tilde{\nabla}(\cdot)$ denotes gradient operator, k is the thermal conductivity, ρ is the density, c_p is the specific heat, h is the heat transfer coefficient, T_{ON} is the initial temperature, and T_f is the fluid temperature. The physical properties are assumed constant for each material of the vessel. The h and T_{ON} are assumed constant.

2.2 Thermomechanics analysis

Obtained $T(r,\theta,z,t)$ for each $t \in (0,\infty)$ fixed, the stress are determined solving the following problem:

$$div\tilde{\sigma} = 0, \tag{2.3a}$$

$$\tilde{\sigma} = \tilde{\sigma}_m + \tilde{\sigma}_{th}, \tag{2.3b}$$

$$\tilde{u}(r,\theta,\pm\tfrac{H}{2},t) = 0, \tag{2.3c}$$

$$\sigma_{rr}(R_i,\theta,z,t) = -p_i, \tag{2.3d}$$

$$\sigma_{r\theta}(R_i,\theta,z,t) = \sigma_{rz}(R_i,\theta,z,t) = \sigma_{\theta z}(R_i,\theta,z,t) = 0, \tag{2.3e}$$

$$\sigma_{rr}(R_e,\theta,z,t) = -p_e, \tag{2.3f}$$

$$\sigma_{r\theta}(R_e,\theta,z,t) = \sigma_{rz}(R_e,\theta,z,t) = \sigma_{\theta z}(R_e,\theta,z,t) = 0, \tag{2.3g}$$

where $\tilde{u}$ denotes the displacement field, $\tilde{\sigma}$ denotes Cauchy stress tensor, $\tilde{\sigma}_m$ is the elastic stress tensor, $\tilde{\sigma}_{th}$ is the thermal stress tensor, p_i is the internal pressure and p_e is the external pressure, and the mechanic properties are assumed constant.

2.3 Fracture mechanics analysis

The linear-elastic fracture mechanics model has been adopted, which is a conservative methodology for this problem. The following hypothesis are additionally assumed:

- Existence of surface cracks in the longitudinal plane of a cylinder, with depths less or equal to 0.25*s*.
- Only Mode I of the crack opening is present.
- The cracks are elliptical following the ASME code's Appendix G, subsection NA, section III as shown in Fig. 2.

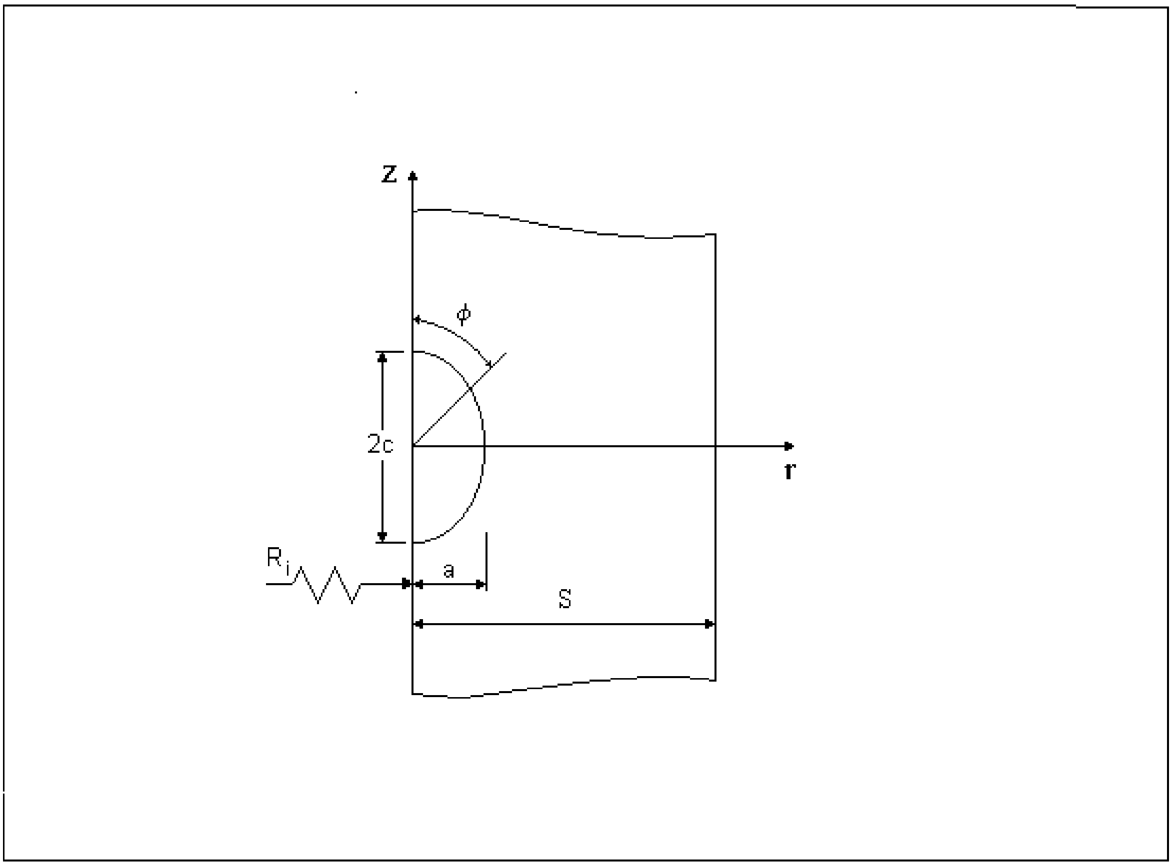

Figure 2. Crack in the longitudinal plane of a cylinder.

- The curve developed on "REG. GUIDE" 1.99 of NRC was adopted for calculating ΔRT_{NDT} .
- The nil-ductility transition reference temperature is determined by using article NB 2331 of the ASME code's subsection NB, section III.
- The place where the crack opening begins determines the criteria to establish the failure, that is: the failure occurs when K_{ic} given on the ASME code's Appendix A, Section XI is overtaken.

  Thus, the fluency F, ΔRT_{NDT} and RT_{NDT} are given by:

$$\Delta RT_{NDT} = [40 + 1000(\%Cu - 0.08) + 5000(\%P - 0.008)]\left(\frac{F}{10^{19}}\right)^{\frac{1}{2}} \tag{2.4}$$

$$RT_{NDT} = (RT_{NDT})_{initial} + \Delta RT_{NDT} \tag{2.5}$$

all temperatures given in F.

Copper percentages (% Cu) and phosphorus (%P) are the same as in the design, which constitutes a conservative assumption. RT_{NDT} is calculated for basic and for weld materials, and the biggest value is chosen.

The expression K_{ic} comes from:

$$K_{ic} = \left\{33.194 + 2.806\, e^{[0.02(T+100-RT_{NDT})]}\right\}1000 \quad \text{psi}\sqrt{\text{in}}\ , \ (T \text{ and } RT_{NDT} \text{ in F}) \tag{2.6}$$

T temperature is evaluated in the crack's tip (ϕ=90°)

The equation (2.6) is valid only when K_{ic} is less or equal to 200.000 psi$\sqrt{\text{in}}$. When the K_{ic} values, obtained through the equation (2.6) are bigger o equal to 200.000 psi$\sqrt{\text{in}}$, then a 200.000 psi$\sqrt{\text{in}}$ value is assumed for K_{ic}.

3. Solution scheme

a) We expand $T_f(\theta, z)$, T_{ON} and $T(r,\theta,z,t)$ in Fourier series as follows:

$$T_f(\theta,z) = T_{f0} + \sum_{l=1}^{\infty}\left[T_{fsl}(z)\cos(l\theta) + T_{fal}(z)\,\text{sen}(l\theta)\right], \tag{3.1}$$

$$T_{ON} = T_{ON} + \sum_{l=1}^{\infty}\left[0\cos(l\theta) + 0\,\text{sen}(l\theta)\right], \tag{3.2}$$

$$T(r,\theta,z,t) = T_0(r,z,t) + \sum_{l=1}^{\infty}\left[T_{sl}(r,z,t)\cos(l\theta) + T_{al}(r,z,t)\,\text{sen}(l\theta)\right], \tag{3.3}$$

b) The temperature profile is obtained by combining two methods. The first one refers to the Euler implicit finite difference scheme; the second, to a methodology described by Zienkiewicz (1979) for the finite element method. Therefore, the Fourier series coefficients, given in (3.3), are determined.

c) The components of stress are also expanded in Fourier series, and again, by following the methodology given by Zienkiewicz (1979), the stress are determined by the finite element method.

d) The stress components $\sigma_{\theta\theta m}$ and $\sigma_{\theta\theta th}$ are fitted by the square minimum method to the polynomial:

$$\sigma_{\theta\theta\mu}(r) = A_0^{\mu} + A_1^{\mu}\left(\frac{r}{s}\right) + A_2^{\mu}\left(\frac{r}{s}\right)^2 + A_3^{\mu}\left(\frac{r}{s}\right)^3 \quad (\mu = m, th) \tag{3.4}$$

where s denotes thickness of the vessel, $\sigma_{\theta\theta m}$ denotes the mechanics stress, and $\sigma_{\theta\theta th}$ denotes the thermal stress, and therefore, the coefficients $A_0^{\mu}, A_1^{\mu}, A_2^{\mu}$ and, A_3^{μ} are determined.

e) The K_{im} and K_{ith} are determined by the following formula used by McGowan and Raymund (1979):

$$K_{i\mu} = \left(\frac{\pi a}{Q}\right)^{\frac{1}{2}}\left[\cos^2(\phi) + \left(\frac{a}{c}\right)^2 \text{sen}^2(\phi)\right]^{\frac{1}{4}}\left\{A_0^{\mu} H_0(\tfrac{a}{c},\tfrac{a}{s},\tfrac{s}{R_i},\phi) + \frac{2}{\pi}\frac{a}{s}A_1^{\mu} H_1(\tfrac{a}{c},\tfrac{a}{s},\tfrac{s}{R_i},\phi) + \right.$$
$$\left. + \frac{1}{2}\left(\frac{a}{s}\right)^2 A_2^{\mu} H_2(\tfrac{a}{c},\tfrac{a}{s},\tfrac{s}{R_i},\phi) + \frac{4}{3\pi}\left(\frac{a}{s}\right)^3 A_3^{\mu} H_3(\tfrac{a}{c},\tfrac{a}{s},\tfrac{s}{R_i},\phi)\right\}, \quad 0 \le \phi \le \frac{\pi}{2} \quad \mu = (m, th) \tag{3.5}$$

where H_0, H_1, H_2, H_3 are the magnification factors shown in Fig. 3 with *a/s*=0.25, 2*c/a*=6, *Ri/s*=10 and Q=1.2426.

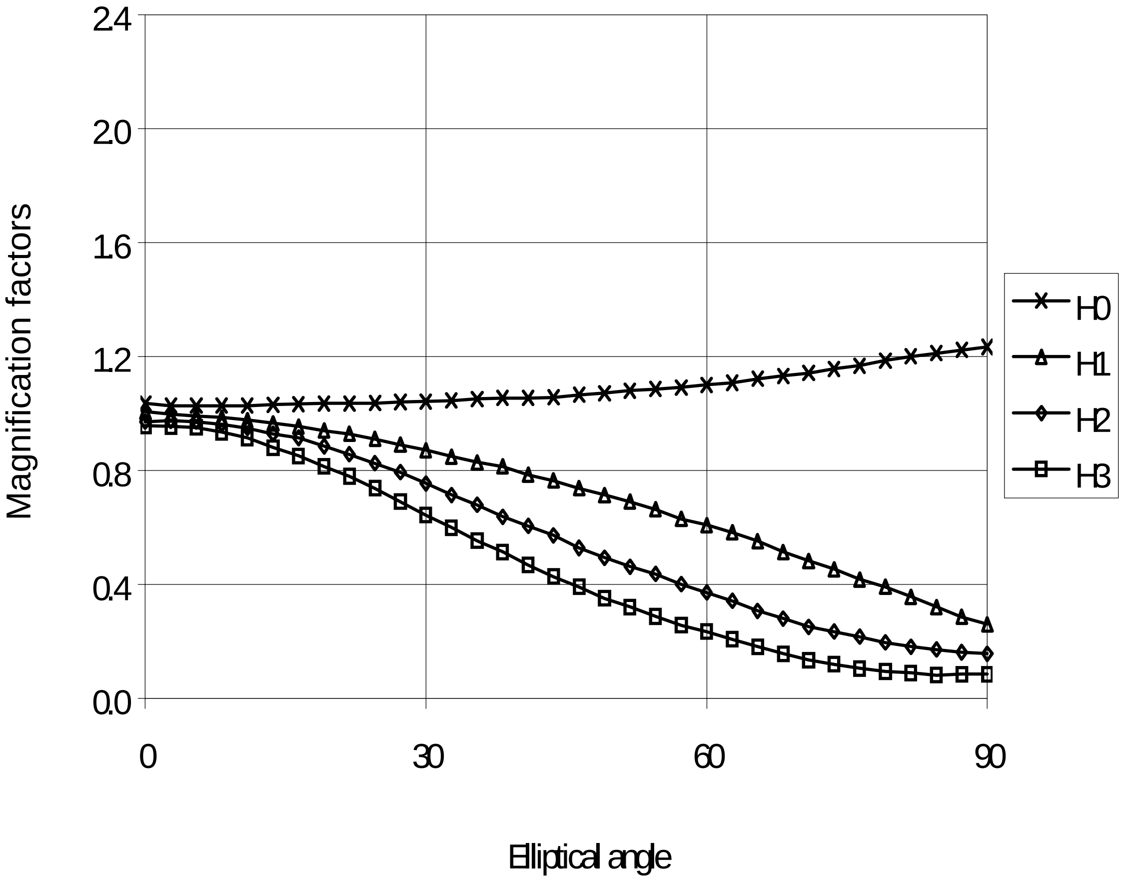

Figure 3. Magnification factors for a elliptical crack in the longitudinal plane of a cylinder.

f) For each temperature $T_f(\theta, z)$ fixed, we define $K_{im}^{\max}$ and $K_{ith}^{\max}$ as being the maximum values among all $\phi \in \left[0, \frac{\pi}{2}\right]$, $t \in (0, \infty)$, $\theta \in [0, 2\pi]$ and $a \in \left(0, \frac{s}{4}\right]$, for K_{im} and K_{ith} respectively.

g) The admissible pressure is determined by:

$$K_{im}^{\max} + K_{ith}^{\max} \leq K_{ic} \tag{3.6}$$

h) The scheme described from (a) to (g) is repeated for each new temperature $T_f(\theta, z)$, and it is finish when the admissible pressure is equal to the safety valve pressure.

4. NUMERICAL RESULTS

Numerical results were obtained for a typical PWR. This data is presented below on tables 1 to 4.

Table 1. Mechanics and thermal properties of vessel

Material	Thickness (m)	Thermal conductivity (J/s m ^oC)	Thermal diffusivity (m^2 /s)	Modulus of elasticity (Mpa)	Thermal expansion ((m/m ^oC)	Poisson's ratio
Cladding	0.003175	18.08	$0.4345\ 10^{-5}$	$1.92\ 10^{5}$	$1.468\ 10^{-5}$	0.3
base	0.1651	46.21	$1.083\ 10^{-5}$	$1.92\ 10^{5}$	$1.468\ 10^{-5}$	0.3

Table 2. Values of h, initial RT_{NDT}, , T_{ON}, safety valve pressure, inner radius, and the ratio of crack depth to wall thickness (a/s)

h (J/s m^2 ^oC)	Initial RT_{NDT} (^oC)	T_{ON} (^oC)	Safety valve pressure (Mpa)	Inner radius (m)	a/s
45429.75	10	287.77	17.133	2.1971	(0,0.25]

Table 3.Values of copper and phosphorus used

Material	Per cent of copper	Per cent of phosphorus
base	0.12	0.017
weld	0.12	0.017

Table 4. Values used for the fluid temperature harmonics

Case	Harmonic	T_{sl}	T_{al}
1	0	T_{f0}	-
2	*l=(1,...,4)*	$\frac{0.05}{2^{(l-1)}}(1.8T_{f0}+32)$	$\frac{0.05}{2^{(l-1)}}(1.8T_{f0}+32)$
3	*l=(1,...,4)*	$\frac{0.10}{2^{(l-1)}}(1.8T_{f0}+32)$	$\frac{0.10}{2^{(l-1)}}(1.8T_{f0}+32)$

Finite-Element Idealization. Bi-linear elements were used constituting a mesh (60×50) on the plane $(r \times z)$ to calculate the temperature's profile; and (20×50) on the plane $(r \times z)$ to calculate stress.

Figures 4 and 5 show an angular dependency of the fluid temperature on the cases under study.

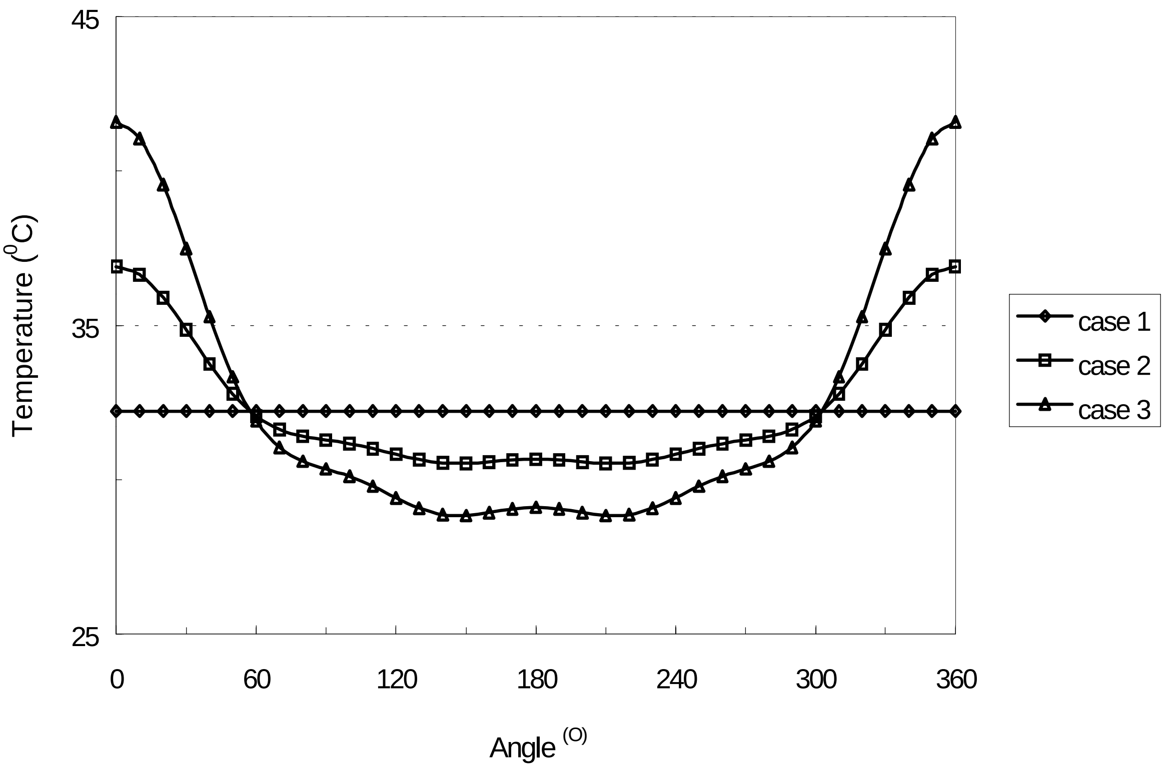

Figure 4. Cold leg temperature expanded on cosine series.

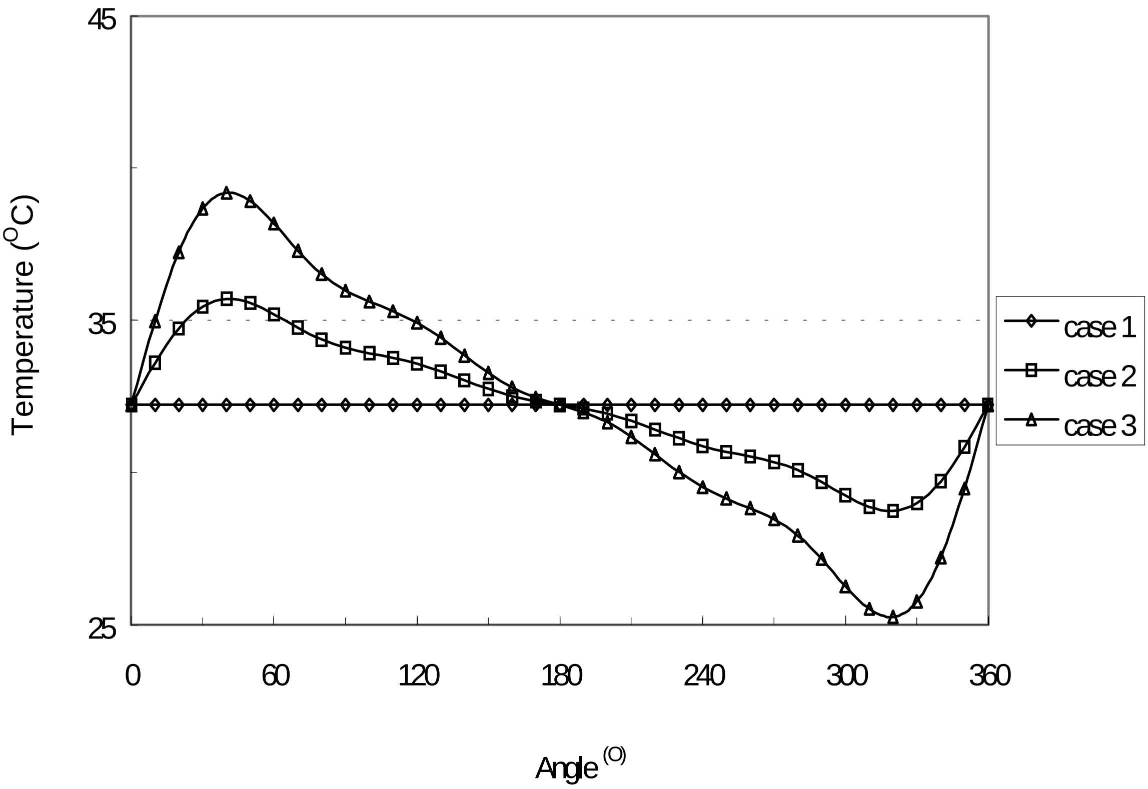

Figure 5. Cold leg temperature expanded on sine series.

The operational bounding curves referred to thermal shock, which were obtained through the data above in each case, are respectively illustrated on Figs. 6 and 7.

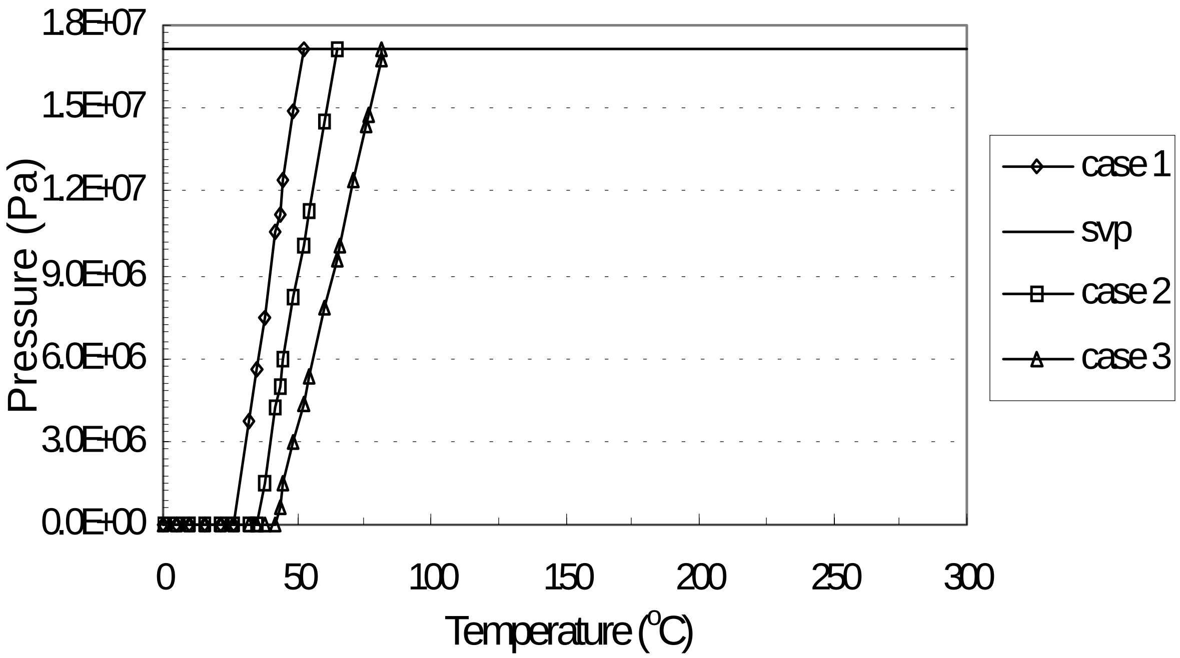

Figure 6. Operational bounding curve for thermal shock with fluid temperature expanded on cosine series.

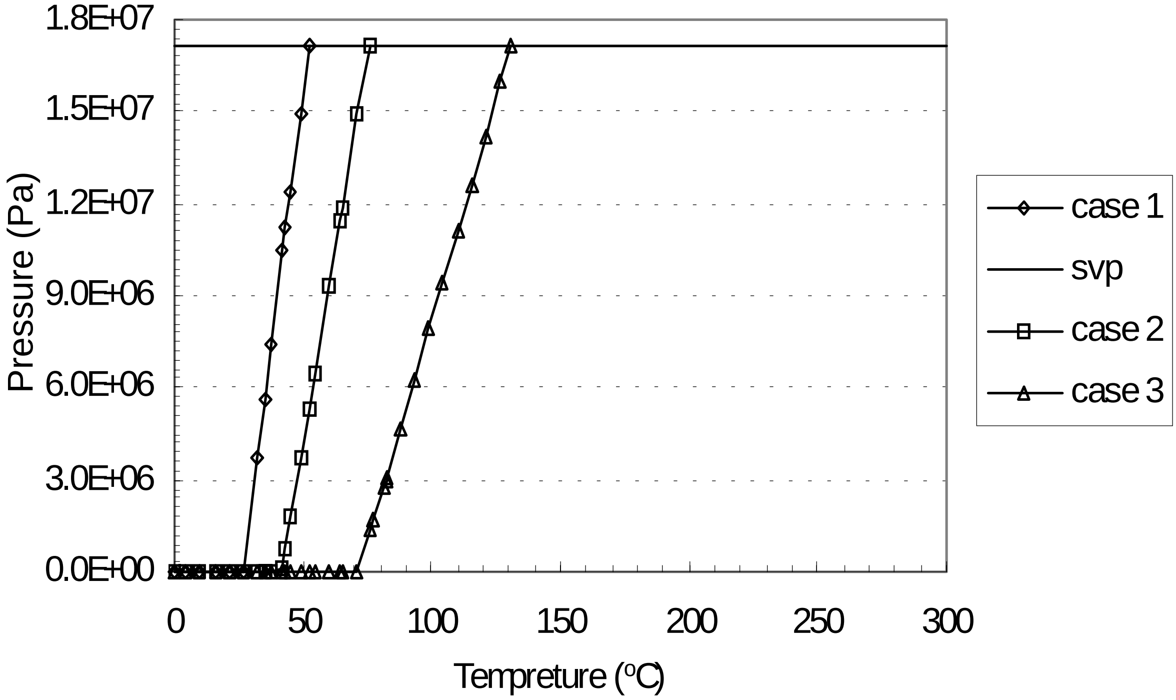

Figure 7. Operational bounding curve for thermal shock with fluid temperature expanded on sine series.

5. CONCLUSION

With the help of a conservative methodology, we modeled the pressure vessel's refrigeration of PWR reactors, considering a given profile of the fluid temperature as an asymmetric profile.

One of the main conservative factors refers to using a maximum heat transference coefficient, refrigerating the reactor by degrees. This method allows high temperature gradients close to the inner wall of the vessel.

Through numerical experiments it was possible to verify the influence of asymmetric refrigeration in the operational curves (pressure against cold leg temperature).

The outcome of this study suggests that a realistic analysis of the vessel should be carried out using a thermohydraulic analysis together with a thermomechanic analysis, in order to validate operational curves as operational bounding curves, which were produced through the methodology proposed by Carmo, Oliveira and Roberty (1984).

REFERENCES

ASME Boiler and Pressure Vessel Code, Section III, "Nuclear Power Plant Component", ASME, New York, 1971.

Carmo, E.G.D, Oliveira, L.F.S. and Roberty, N.C., Prevenção contra fratura frágil em vaso de pressão de reatores PWR em presenca de choque térmico pressurizado, Proceedings of the *3° Simposio Brasileiro Sobre Tubulações e Vasos de Pressão*, October 29-31, Salvador-Bahia, pp. 499-516, 1984.

McGowan, J.J. & Raymund, M., 1979, Stress Intensity Factor Solutions for Internal Longitudinal Semiellipticall Surface Flaws in a Cylinder Under Arbitrary Loading, STM STP 677.

Timoshenko, S.P. and Goodier, J.N., 1951, Theory of Elasticity, 2nd Ed., McGraw-Hill Book Company, New York.

Zienkiewicz, O.C., 1979, The Finite Element Method, 3rd Ed., McGraw-Hill Book Company (UK) Limited.